NANO-PATTERNING OF MOTOR PROTEINS TO CONTROL NUMBER OF KINESIN MOLECULES TRANSPORTING A SINGLE MICROTUBULE

Taikopaul Kaneko, Hirofumi Shintaku, Hidetoshi Kotera, and Ryuji Yokokawa
Department of Micro Engineering, Kyoto University, Japan

ABSTRACT

We propose a nano-patterning method to control the number of kinesin motors involving in a collective transport of a single microtubule (MT) filament. We fabricated Au nano-pillar array on a thermally oxidized silicon substrate. SiO_2 surface was selectively coated with poly(ethylene glycol) (PEG) self-assembled monolayer (SAM) and was rendered inert to protein adsorption. Streptavidin was immobilized only on Au nano-pillars to immobilize kinesin-1 motors. MTs glided on the top of kinesin-1-immobilized Au nano-pillars, where the number of motors and the spacing between motors transporting a single MT were defined. Our patterning method helps to study how the collective dynamics of multiple motors are regulated by the number of motors and the arrangement of motors with an in vitro assay.

INTRODUCTION

Kinesin and dynein proteins are important molecular motors that transport various cargos such as intracellular vesicles and organelles. Recent works revealed that molecular motors usually work together as a team in living cells [1], [2]. Collective dynamics of multiple motors depends on mechanical properties of individual motors, the number of motors, and the arrangement of these motors.

The processivity of individual motors is one of the most important property that affects the collective dynamics. Kinesin-1 is a highly processive motor, which can take hundreds of steps before detaching from a MT. Both in vivo and in vitro studies showed the number of kinesin-1 motors had little influence on the velocity and run length of collective transport [3]–[6]. Kinesin-5, kinesin-14 and dynein are nonprocessive motors which detach from a MT after a single step [7]. Collective dynamics of these non-processive motors enables to produce larger run length and velocity than that can be achieved by a single non-processive motor [3], [8]. This suggests nonprocessive motors can transport cargos more cooperatively than processive motors.

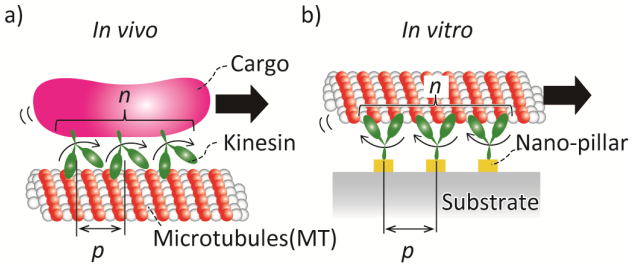

Figure 1 Schematic illustration of transport of cargos by multiple motor proteins. (a) In vivo, motors attach on a cargo and transport it together along a microtubule (MT). (b) In vitro, motors are immobilized onto substrates and transport a MT, mimicking in vivo transport. We selectively immobilized kinesin on Au nano-pillars and controlled the number of motors, n, and the spacing between motors, p, which transport a single MT.

Most functions of non-processive motors in vivo are shown as a team. However, the overexpression of these motors has negative influences on their functions in living cells. Kinesin-5 and kinesin-14 show aberrant overexpression in various cancer cells and are identified as oncogenes[9], [10]. Although some studies proposed these motors can be a potential cancer drug target, how the overexpression of motors causes cancer is still incompletely understood due to the lack of knowledge about the effect of the increasing number of motors on their collective dynamics.

Not only the number of motors but also the arrangement of motors affects their collective dynamics has been reported. Axonemal dyneins are arranged in a repeating pattern along MTs of cilia and flagella, and power the sliding motions between outer doublet MTs to drive ciliary and flagellar motility. This periodic arrangement is regulated by a molecular ruler and its repeating period is exactly 96 nm or 24 nm, which is a multiple of 8 nm (the length of tubulin dimer) [11]. A number of studies have addressed that in the absence of molecular rulers, periodic alignment of dynein is disrupted and this brings dysfunction of cilia [12]. However, further investigation is necessary to understand whether only the periodic alignment of dynein is required or the periodic spacing is also essential to the collectively generated force.

In order to understand how the number and the arrangement of motors affect their collective dynamics, we controlled these two parameters for various motors by nano-fabrication. These parameters were previously controlled using DNA origami [3], [13]. Although such bottom-up methods control the spacing between motors, the controllable number of motors is limited up to 10 motors, which is smaller than that of in vivo motors working together, 10 - 100.

To overcome this limitation, we controlled the number and the arrangement of motors by top-down approach. As the integration of top-down approach and motor proteins, target molecules have been transported in microchannels by motor proteins patterned on the channel surface [14], [15]. Advancing these technologies, we patterned kinesin-1 motors on fabricated Au nano-pillars and controlled the number and the arrangement of motors independently. Our patterning method enabled to control the number of motors from 1 up to 200 molecules, which is similar with the number of motors working together in vivo. Furthermore, this method enabled to control the spacing between motors from 100 nm to 10 μm and arrange motors with various patterns. Since kinesin-1 motors can be replaced with various other motors such as Ncd and

Eg5, our proposed top-down patterning method can be a platform to study cooperativity of motor proteins.

EXPERIMENTAL METHODS

Figure 1 shows the schematic illustration of transport of cargos by multiple motors and patterned kinesin-1 molecules. Au nano-pillar array was fabricated on an Si/SiO_2 substrate and kinesin-1 motors were selectively immobilized on Au nano-pillars. These patterned kinesin-1 motors transport MTs with the defined number of motors, n, and the spacing (or pitch) between motors, p, involving a single MT transport. The spacing between pillars, p, can be designed and the number of motors transporting an MT can be calculated by dividing the MT length by p.

Au nano-pillar arrays were fabricated by electron beam (EB) lithography and lift-off process. Figure 2a shows designs of nano-pillars. The 50-nm diameter pillars were arranged hexagonally with 200-nm or 500-nm pitch. The fabrication process is presented in Figure 2b. A positive EB resist (ZEP-520A, ZEON) with a thickness of 110 nm was patterned by high-resolution EB lithography (F7000, Advantest). The thermal evaporation was used to deposit a 20-nm-thick Au layer and a 3-nm-thick Cr adhesion layer. The subsequent lift off was done by soaking in *N,N*-Dimethylacetamide for 10 minutes and by sonication in acetone for 10 minutes.

SiO_2 surface was selectively coated with PEG-SAM to repel proteins (Figures 3a, b). To form PEG-SAM, the substrate was submersed in 3:1 Piranha solution for 10 min. Then, the substrate was rinsed three times in deionized water (DIW) and was dried with nitrogen. The substrate was heated to 180°C for 5 minutes and was immersed in the PEG solution under nitrogen atmosphere for at least 24 hours. The solution consists of 3 mM 2-[methoxypoly-(ethyleneoxy)propyl]-trimethoxysilane and 0.2%$_v$ HCl (36%) in toluene. Following rinsing process in toluene, ethanol, DIW, and sonicated in DIW for 2 minutes, the substrate was baked at 120°C for 1 hour to anneal grafted PEG-SAM. The substrate was stored in nitrogen atmosphere until use.

To evaluate the protein-repelling PEG-SAM ability and selective PEG-SAM coatings, six kinds of substrates were prepared: 1) glass, 2) bare SiO_2, 3) Au-coated SiO_2, 4) PEG-SAM-coated SiO_2, 5) Au-coated SiO_2 immersed in a PEG-SAM solution, 6-8) PEG-SAM-coated Au

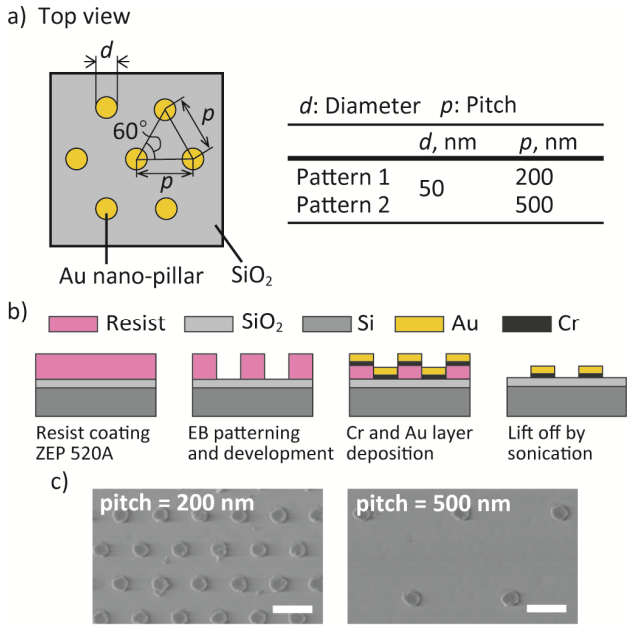

Figure 2 Fabrication of Au nano-pillars. (a) Designs of nano-pillars. Nano-pillars were arranged hexagonally (left). Two variation of designs were prepared (right). (b) Fabrication process of nano-pillars. Au nano-pillars were fabricated by EB lithography and lift-off process. (c) SEM images of fabricated nano-pillars with 200-nm (left) and 500-nm (right) pitches. Scale bar = 200 nm.

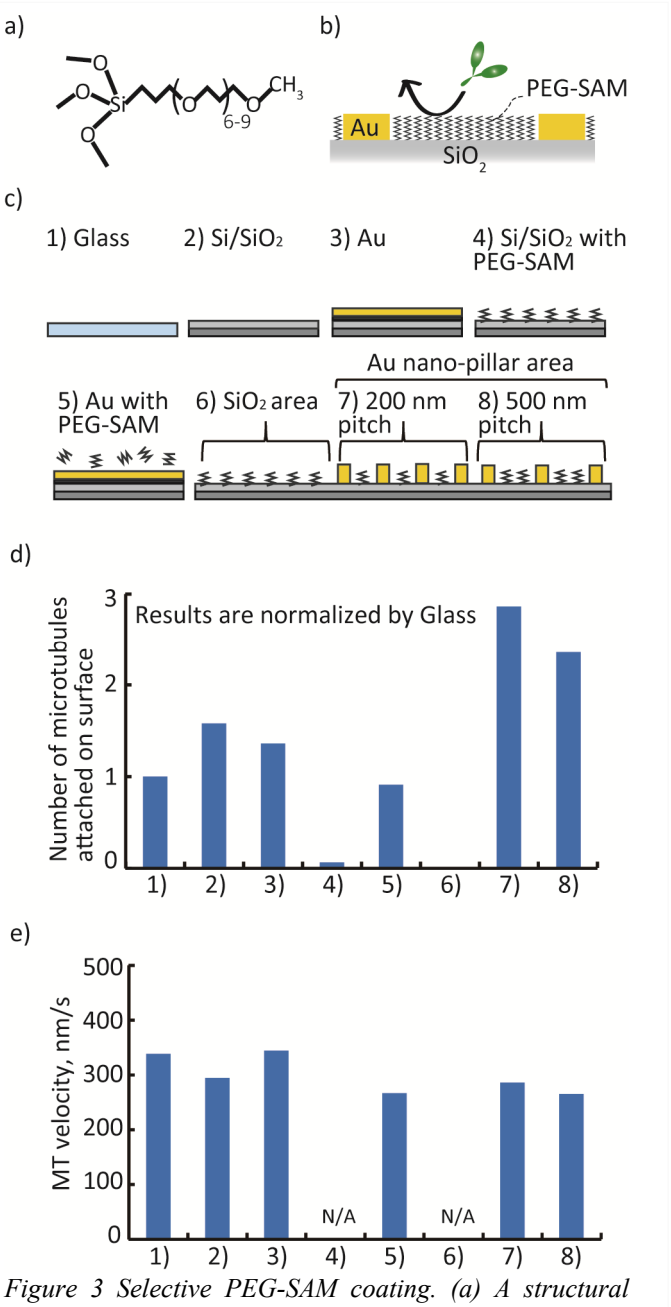

Figure 3 Selective PEG-SAM coating. (a) A structural formula of PEG-SAM. (b) PEG-SAM-coated SiO_2 surface has protein-repelling property. (c) Six kinds of samples were prepared to evaluate the PEG-SAM protein-repelling property and its selective coating. (d) The number of MTs attached on the surface for each sample. Results were normalized by the number of MTs on a glass. (e) MT gliding velocity for each sample.

nano-pillar substrate (Figure 3c). Six flow chambers were constructed by bonding a substrate to coverslips with double-sided tapes. First, the streptavidin solution was introduced. Streptavidin molecules absorbed on surfaces because their affinity to glass, SiO_2, and Au surface without PEG-SAM. Then, biotin-conjugated kinesin-1 solution was introduced, and kinesin-1 motors attached to the surface by streptavidin-biotin linkage when streptavidin is coated on the surface. Fluorescently-labeled MT solution and ATP solution were introduced to launch MT gliding. Then, the number of attached MTs and MT gliding velocity were measured. Results of the number of MTs were normalized by that on a glass.

Motility assay of MTs were conducted on kinesin-1-immobilized Au nano-pillars. Figure 4a shows schematic illustration of patterned kinesin-1 on Au nano-pillars. PEG-SAM was selectively formed on SiO_2 surface as described above. Streptavidin was immobilized on Au surface by nonspecific absorption. Biotin conjugated kinesin-1 motors were immobilized on Au surface by biotin-streptavidin specific binding. Fluorescence MTs were flowed into the flow cell and MT motility were launched by introducing 1 mM ATP solution. The dependency of MTs velocity on the number of and the spacing between motors were measured.

MTs were observed by a fluorescence microscopy. Optical images were stored as sequential image files with a CMOS camera. The number of MTs attached on a surface was manually counted using ImageJ software. MT velocity was calculated from trajectories of MT tips which was obtained with a Mark2 image analysis software. The length of MTs was measured by ImageJ software and the number of motor proteins moving the single MT was calculated by dividing the length of MTs by the pitch of pillars.

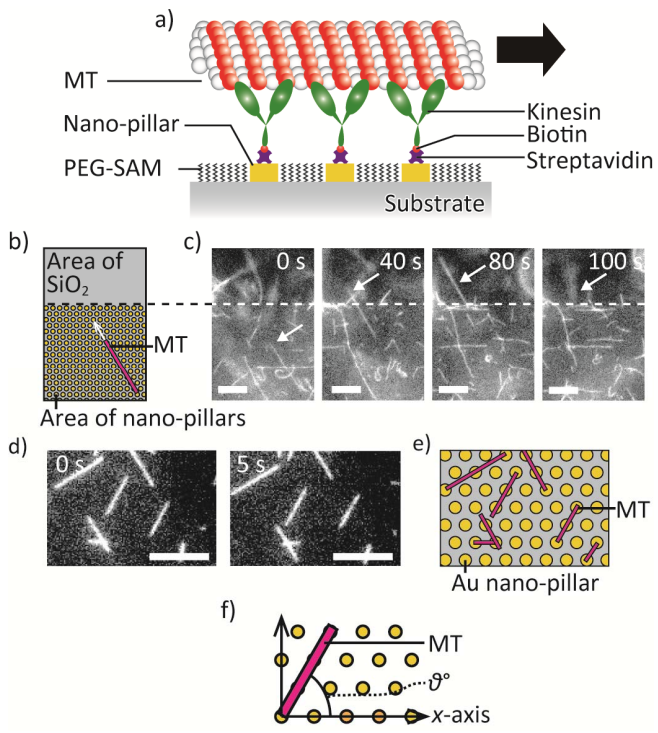

Figure 4 MT motility assay on patterned kinesin-1 molecules. (a) Schematic illustration of an MT gliding on patterned kinesin-1 molecules. (b) Schematic illustration of MTs gliding on Au nano-pillar regions. (c) Sequential images of gliding MTs. When MTs entered into PEG-SAM-coated area, they detached from the surface. White arrows indicate the motion of typical MT. Scale bar = 10 μm. (d) Typical florescence images of MTs on nano-pillars. Scale bar = 10 μm. (e) Schematic illustration of MTs on nano-pillars shown in (d). MTs were aligned along the line of pillars. The diameter and pitch of pillars are not in scale. (f) Definition of the angle of MTs on nano-pillars.

RESULTS AND DISCUSSION

Fabrication of Au Nano-pillars

From SEM images shown in Figure 2c, we measured *d* of fabricated Au nano-pillars. The diameter of pillars were 75.9 ± 3.8 nm (N = 20, Mean ± S.D.). In addition, we found almost no lack of pillars. These results suggested Au nano-pillars arrays were successfully fabricated.

Selective PEG-SAM Coating

As shown in Figure 3d, almost no MT attached on the PEG-SAM coated SiO_2 surface. This indicates PEG-SAM prevented kinesin-1 from attaching on the surface. In contrast, many MTs attached and glided on an Au-coated substrate even when the substrates had been immersed in the PEG-SAM solution. It indicates PEG-SAM was not

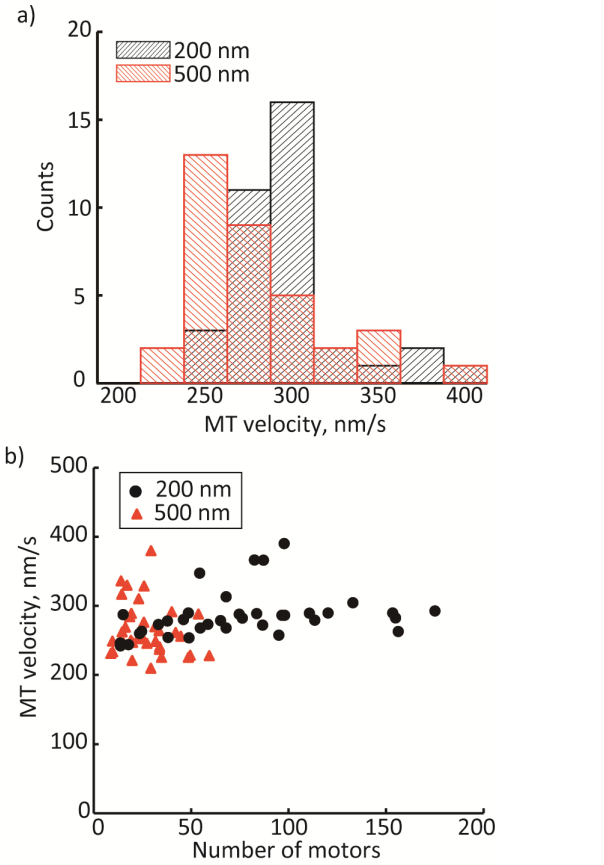

Figure 5 Dependency of MT velocity on the spacing between motors and the number of motors. (a) The histogram of MT velocity gliding on kinesin-1 motors with 200 nm spacing (gray box) and 500 nm spacing (red box). (b) The dependency of MT velocity on the number of kinesin-1 motors.

formed on Au surface. Therefore, PEG-SAM was selectively formed on SiO_2 surface and prevented non-specific absorption of proteins. MT gliding velocity on an Au-coated substrate immersed in PEG-SAM was similar to that on a kinesin-1-coated glass surface (a control experiment), suggesting that kinesin-1 molecules immobilized on Au surface were not denatured. We found no MTs attached on PEG-SAM-coated SiO_2 region of the nano-pillar substrate (Figure 3d, e).

Gliding Assay on Au Nano-Pillars

Figure 4c shows sequential images of MT gliding on the top of kinesin-1-immobilized pillars. An MT (indicated by white arrow) glided on Au nano-pillar region (Figure 4b). When the leading tip of the MT exit the nano-pillar region, the tip started detaching and finally completely detached from the surface. This result indicates kinesin-1 motors bound only on Au nano-pillars not on SiO_2 region. Figure 4d is typical fluorescence images of MTs gliding on kinesin-1-immobilized nano-pillars. Figure 4e shows relative position of MTs on nano-pillars in Figure 4d. Most of MTs glided along the nearest-neighbor collinear pillars. Small population of MTs glided on the line of nearest-neighbor collinear pillars. To quantitatively analyze relative position of MTs on nano-pillars, the orientations of MTs were measured. The line of nearest collinear pillars was set as *x*-axis (Figure 4f) and the angle between *x*-axis and MTs were measured (θ, $0° \leq \theta \leq 90°$). 58.7% MTs were within $0° \leq \theta \leq 5°$ or $55° \leq \theta \leq 65°$, 22.9% MTs were within $25° \leq \theta \leq 35°$ or $85° \leq \theta \leq 90°$, and 18.3% MTs were other degree. This indicates kinesin-1 motors were successfully immobilized only on nano-pillars.

Collective Transport by Multiple Kinesin-1 Motors

Figure 5a shows the dependency of MT gliding velocity on the spacing between kinesin-1 motors. MT gliding velocity on motors with 500-nm spacing was smaller than that on motors with 200-nm spacing, indicating large spacing may decrease the velocity of collective transport by kinesin-1 motors. Figure 5b shows the dependency of MT velocity on the number of motors involving in transport of a single MT. The number of motors had no effects on the MT gliding velocity, suggesting kinesin-1 molecules dose not cooperate at 10 - 200 motors.

CONCLUSION

To study the cooperativity of motor proteins, we proposed a method to control the number of motors transporting a single MT and the spacing between motors. Au nano-pillars were fabricated and kinesin-1 molecules were immobilized only on Au nano-pillars. This selective patterning method enabled to evaluate the dependency of MT gliding velocity on the number of kinesin-1 and spacing between kinesin-1 molecules. Other motor proteins, including Eg5, CENP-E, Ncd and dynein, can be replaced with kinesin-1 in the same molecular system. Therefore, our proposed molecular patterning method can be utilized as an assay platform to study the cooperativity of multiple motors.

ACKNOWLEDGEMENTS

This research was partially supported by JSPS KAKENHI Grant Number 25709018 and Kyoto University Nano Technology Hub in "Nanotechnology Platform Project" sponsored by the Ministry of Education, Culture, Sports, Science and Technology (MEXT), Japan. We thank Dr. Kenya Furuta, National Institute of Information and Communications Technology, Kobe, Japan for discussion and Mark2 image analysis software.

REFERENCES

[1] V. Fridman, *et al.*, *Journal of Cell Science*, vol. 126, 18, pp. 4147–59, 2013.

[2] C. Hentrich and T. Surrey, *Journal of Cell Biology.*, vol. 189, no. 3, pp. 465–480, 2010.

[3] K. Furuta, *et al.*, *PNAS*, vol. 110, no. 2, pp. 501–506, 2013.

[4] K. Svoboda, *et al.*, *Nature*, vol. 365, no. 6448, pp. 721–727, 1993.

[5] P. Bieling, *et al.*, *EMBO Reports.*, vol. 9, no. 11, pp. 1121–7, 2008.

[6] C. Leduc, *et al.*, *PNAS*, vol. 104, no. 26, pp. 10847–52, 2007.

[7] R. J. Stewart, *et al.*, *European Biophysics Journal*, vol. 27, no. 4, pp. 353–360, 1998.

[8] Y. Shimamoto, *et al.*, *Developmental Cell*, vol. 34, no. 6, pp. 669–681, 2015.

[9] B. L. Theriault, *et. al.*, *PLOS One*, vol. 9, no. 3, 2014.

[10] S. Ding, *et al*, *International Journal of Urology*, vol. 18, no. 6, pp. 432–438, 2011.

[11] M. Owa, *et al.*, *PNAS*, vol. 111, no. 26, pp. 9461–6, 2014.

[12] R. Hjeij, *et al.*, *American Journal of Human Genetics.*, vol. 95, no. 3, pp. 257–274, 2014.

[13] N. D. Derr, *et al.*, *Science*, vol. 338, pp. 662–666, 2012.

[14] N. Isozaki, *et al., Scientific. Reports*, vol. 5, p. 7669, 2015.

[15] K. Fujimoto, *et al., Lab on a Chip*, vol. 15, pp. 2055–2063, 2015.

CONTACT

*T. Kaneko, tel: +81-75-383-3687;
kaneko.taikouporu.75x@st.kyoto-u.ac.jp